Metagenomic Profiling of Ocular Surface Microbiome Changes in Meibomian Gland Dysfunction

Fuxin Zhao
Wenzhou Medical University
Dake Zhang
Beijing Institute of Genomics Chinese Academy of Sciences
Chaoxiang Ge
Wenzhou Medical University
Lei Zhang
deepbiome CO., Ltd
Peter S Reinach
Wenzhou Medical University
Xiangjun Tian
University of Texas MD Anderson Cancer Center
Chengcheng Tao
Beijing Institute of Genomics Chinese Academy of Sciences
Zhelin Zhao
Wenzhou Medical University
Chenchen Zhao
Wenzhou Medical University
Wenjie Fu
Wenzhou Medical University
Changqing Zeng
Beijing Institute of Genomics Chinese Academy of Sciences
Wei Chen (chenweimd@hotmail.com)
Wenzhou Medical University https://orcid.org/0000-0002-4040-6721

Research

Keywords: meibomian gland dysfunction; microbiome; metagenomics; metabolism; pathogen; benzoate degradation.

Posted Date: April 21st, 2020

DOI: https://doi.org/10.21203/rs.3.rs-22876/v1

Abstract

Background: Ocular surface microbiome changes can affect meibomian gland dysfunction (MGD) development, which in turn may increase the risk of tissue infection. To delineate what these changes are, we used shot-gun metagenomic analysis to determine if there are differences between the microbial communities in ocular sites surrounding the meibomian gland in healthy and patients afflicted with MGD. This comparison entailed comparing the microbe content in different microbiomes of the eyelid skin, conjunctiva and meibum with those from the same locations in healthy individuals (HC) and those with this disease.

Results: The meibum bacterial content of these microbiomes was different in these two different types of individuals. Almost all of the most significant taxonomic changes in the meibum microbiome of these individuals with MGD were also present in their eyelid skin, but not in the conjunctiva. Such site-specific microbe pattern changes accompany increases in the gene expression levels controlling carbohydrate and lipid metabolism. Most of the microbiomes in MGD disease possess a microbe population capable of metabolizing benzoate. Interestingly, microbe preponderance seemed to be less in patients afflicted with more severe MGD. Nevertheless, pathogens known to underlie ocular infection were evident in these patients. In meibum samples from HC, *Pseudomonas fluorescens* was present in more than 90% of the samples. *Cupriavidus metallidurans* and *Pseudomonas putida* had a positive rate over 50%. MGD meibum contained instead an abundance of *Campylobacter coli*, *Campylobacter jejuni*, and *Enterococcus faecium* pathogens, which were almost absent from HC. Functional annotation indicated that in the microbiomes of MGD meibum their capability to undergo chemotaxis and display immune evasive virulence and mediate Type IV secretion was different than that in the microbiomes of meibum isolated from HC.

Conclusions: MGD meibum contained distinct microbiota different from HC, and MGD meibum microbiome community population was much smaller than in the HC group. Profiling differences in the meibum microbiome makeup between HC and MGD patients may uncover unique targets for improved treatment of this disease.

Background

Meibomian gland dysfunction (MGD) is the most prevalent cause of evaporative dry eye disease, Rabensteiner et al found that 70.3% of dry eye patients exhibited signs of this disease [1]. It is characterized by chronic, diffuse meibomian gland abnormality, usually resulting from obstruction of the terminal duct of the meibomian gland and/or abnormal changes in the quality and quantity of glandular secretion by this gland. Such dysfunction can result from glandular losses, opening abnormalities at the eyelid margin blocking meibomian gland release onto the ocular surface [2, 3]. Meibomian glandular lipid secretory abnormalities or lipid component changes are major manifestations of MGD. Until now, its underlying pathogenesis is poorly understood.

Meibomian gland lipid secretions are essential for preventing ocular surface desiccation since they reduce tear film evaporation by spreading over the aqueous covering the ocular surface. In addition, they are an important component of the ocular surface antibacterial system because they form a barrier, which protects the eyes from microbial infections. In MGD patients, changes in the lipid component of the meibum secreted by the meibomian gland, include increases in certain fatty acids, *etc* [4–7]. Such changes can alter the physical properties of the tear film and also trigger receptor mediated cell signaling events that comprise pathological sequelae in this disease. The microbiome and ocular immune functional competence stems from adapting to the challenges that eyes encounter as a consequence of constant exposure to numerous environmental challenges. There is extensive interest in identifying the host-microbial interactions in this ecosystem since such insight can potentially lead to the design of novel agents that are more selective in therapeutic management of ocular diseases in a clinical setting.

Meibomian glandular lipid abnormalities are believed to be associated with changes in the makeup of ocular surface microbial populations [8]. The accumulation of lipids resulting from the blockage of the meibomian gland duct limits its bactericidal capability, which in turn heightens proliferation of ocular surface microorganisms [2]. Bacterial culturing of the ocular surface of MGD patients demonstrated that there are multiple strains exhibiting significant potential pathogenic roles. They include coagulase-negative staphylococci (mainly *Staphylococcus epidermidis*), *P. acnes*, coryneform bacteria, and *Staphylococcus aureus* [9]. It is particularly noteworthy that the cholesterol esterase and fatty wax esterase activities of *Staphylococcus epidermidis* are essential in promoting the pathogenesis of MGD [10, 11]. Pathogen identification is crucial for infection control. Nevertheless, extensive efforts are still needed to more extensively characterize the resident pathogens responsible for ocular diseases.

In recent years, identifying the changes in the microbial population on the human body surface have become areas of intense interest in numerous different research fields studying disease processes. Novel data analysis of methodology is accumulating along with more improved metagenomic research procedures [12–14]. Considering the risks of ocular infection by any of the different aforementioned bacteria, there is a pressing need to gain additional insight into the content of ocular surface microbiomes. Diverse efforts have been employed to characterize the microbes inhabiting this domain in a pathological condition [15–18]. Nevertheless, most progress has been restricted to focusing on the composition of the microbial population using 16S rDNA/rRNA sequencing to characterize the microbiomes in ocular sites. There are limited studies adopting untargeted sequencing of all microbes present in meibum using shotgun metagenomics.

Here, we collected samples from meibum, eyelid skin and conjunctiva of MGD patients and healthy individuals. Shotgun metagenomic analysis was performed involving next generation sequencing to characterize pathogens within these sites, identify functional changes related to MGD development and interrelationships among these different microbial populations at these three different ocular sites. Site specific differences were identified on the ocular surface between the microbial populations in the meibum of MGD and healthy individuals. Novel targets were uncovered that are possibly relevant in improved management of this disease in a clinical setting.

Results

Decreased microbial abundance in MGD meibum and eyelid skin

In all, we enrolled 61 MGD patients and 15 volunteers as healthy controls (HC) (Fig. 1, Table S1). They provided DNA samples from swabs of meibum from the eyelid skin and conjunctiva following our previous procedure (Fig. 1, Method). After performing quality control and removing host sequences, 117 metagenome datasets were obtained. Each dataset contained over 100 K sequencing reads for metagenome assembly and subsequent annotations (Table S2). In taxonomic profiling, taxa were determined based on nucleic acid annotation and marker gene presence, respectively (Figure S1). In *de novo* assembly, each dataset had 32,692 contigs on average, with their mean length ranging from 225 bp to 528 bp (Table S3).

In MGD meibum, microbial populations having the same phylum were preponderant at the three ocular sites: *Proteobacteria*, *Actinobacteria*, *Firmicutes*, *Bacteroidetes*, and *Negarnaviricota* (Fig. 2A). At the genus level, the predominant genera at the three ocular sites are Pseudomonas, Cutibacterium, Campylobacter, Corynebacterium, Rubrobacter. At the species level, Cutibacterium acnes, Pseudomonas azotoformans, Rubrobacter xylanophilus, Campylobacter coli, Pseudomonas fluorescens were preponderant (Fig. 2A). Samples were clustered into distinct groups according to different levels of taxonomic classification and their disease status (Fig. 2B, Figure S1). As expected, the eyelid skin microbiome had the highest community richness, whereas conjunctival flora was sparse. In MGD patients, their meibum microbiome community population was much smaller than in the HC group (chao1, Fig. 2C), while their community diversities were similar (Shannon, Fig. 2D; Simpson, Fig. 2E). This population decline was attributable to decreases in the abundance of the more preponderant microbes in these patients. Interestingly, alpha diversity was similar in the meibum and eyelid skin microbiomes (Fig. 2C-E).

Changes in the microbial community were observed in the microbiomes of MGD meibum and eyelid skin at different taxonomic classification levels (Fig. 3A-C). Comparing to HC the most significant microbial change at the phylum level in MGD meibum was the significantly decreasing abundance of *Proteobacteria* ($\log_2$FoldChange = -4, adjusted *p*-value = 2.8×10^{-15}, Table S4), which was also seen in the MGD eyelid skin microbiome (Fig. 3D, Table S5). A comparison of the MGD and HC groups shows that the top ten genera whose abundance was not the same, and they were present at higher levels in MGD meibum. These genera included *Rubrobacter*, *Novibacillus*, *Campylobacter*, *Geobacillus*, *Sphingomonas*, *Corynebacterium*, *Sphingobium, Pedobacter*, *Fictibacillus*, and *Enterococcus* ($\log_2$FoldChange = 3 ~ 14, adjusted *p*-value < 1×10^{-6}, Table S4). Among these genera, the same changes were observed in the top three and *Corynebacterium* in the eyelid skin microbiome, while greater abundance of *Geobacillus*, *Sphingomonas*, *Sphingobium, Pedobacter*, *Fictibacillus*, and *Enterococcus* was specific to the microbiome of the MGD meibum. At the species level, the top ten were *Rubrobacter*

xylanophilus, *Novibacillus thermophilus*, *Sphingomonas sp. SL9*, *Campylobacter coli*, *Campylobacter jejuni*, *Sphingomonas panacis*, *Sphingomonas hengshuiensis*, *Rubrobacter radiotolerans*, *Sphingobium sp. SYK-6*, *Sphingomonas wittichii*, all of them were more abundant in MGD samples ($\log_2$FoldChange = 5 ~ 14, adjusted *p*-value < 1×10^{-9}, Table S3). Among them, only *Sphingobium sp. SYK-6* was only more abundant in the MGD meibum whereas the other 9 species were also more preponderant in the microbiomes of the MGD eyelid skin (Fig. 3F).

At the genus and species levels, there were other changes that were highly significant (adjusted *p*-value < 0.005, Benjamini-Hochberg, Fig. 3E-F) in the MGD meibum (genus,47; species,185) than in the eyelid skin (genus, 31; species, 99). Specifically, all of the taxa that were common to the two aforementioned sites were more abundant in MGD patients than HC volunteers. However, in some strains of the *Pseudomonas genus* there were species with altered abundance that were specific to MGD meibum. These strains *account* for 88% (44/50, green, Fig. 3F) of the species with decreased abundance in the MGD meibum at this significance level. Nevertheless, two other species of *Pseudomonas*, *P. yamanorum* and *P. virus SM1* (bold italic, Fig. 3F), are exceptions, whose abundance in meibum was greater in MGD than in HC.

Pathogen Preponderance In Meibum And Disease Status

In HC samples, 968 different strains of pathogens were detected (Method), whereas MGD samples contained 2400 pathogens (pathogen, Table S1). However, on the average, the population of each individual pathogen in the MGD group at the two sites (conjunctiva and eyelid skin) was smaller than in the HC group (Mean, MGD 26 vs HC 37, $p = 0.02$, Welch *t*-test). Interestingly, the MGD meibum also had far fewer pathogens than that in the HC group (Mean, MGD 13 vs HC 36, $p = 0.0014$, Welch *t*-test, Figure S2A). In addition, in the MGD patients, the magnitude of decreases in the number of different types of pathogens were slightly correlated with increases in disease severity ($p = 0.065$, Welch *t*-test, Figure S2B). Additionally, there was either no gender or age difference between the numbers of pathogens in the meibum and those at two ocular sites (conjunctiva and eyelid skin) between the MGD and HC groups (Figure S2C and Figure S3).

Twenty pathogens were identified whose positive rate was different in MGD patients from that in the HC ($p < 0.05$, Welch *t*-test, Table 1, Figure S2D). Furthermore, 28 pathogens were detected whose positive rate was greater than 10% in the meibum samples (Table 2, Figure S2E). The most preponderant pathogens in all meibum samples were *Pseudomonas fluorescens*, in over 90% of the samples (Table 2, Figure S2E), *Cupriavidus metallidurans* (76%) and *Pseudomonas putida* (52%). Nevertheless, only *Pseudomonas fluorescens* was present in 90% of the MGD and 100% of the HC samples ($p = 0.044$, Table 2). Pathogens whose positive rate was much higher in MGD than in HC meibum were *Campylobacter coli* ($p = 4.4 \times 10^{-10}$, Welch *t*-test, Table 1), *Campylobacter jejuni* ($p = 1.2 \times 10^{-8}$, Welch *t*-test), and *Enterococcus faecium* ($p = 8.3 \times 10^{-8}$, Welch *t*-test). Furthermore, their abundance was more than 16-fold higher in the MGD than in the HC meibum (adjusted *p*-value < 2×10^{-8}, Table S4). Additionally, *Pseudomonas aeruginosa* ($p = 4.8 \times 10^{-6}$), *Pseudomonas mosselii* ($p = 1.4 \times 10^{-4}$, Welch t-test), *Escherichia coli* ($p = 0.001$, Welch *t*-test),

Stenotrophomonas maltophilia (p = 0.008, Welch t-test), and *Neisseria sicca* (p = 0.016, Welch t-test) had a lower positive rate in the MGD meibum and samples from the eyelid and conjunctiva.

Table 1
Pathogens with differential positive rate in meibum between MGD and HC

Pathogen	MGD (n = 47*)	HC (n = 11*)	*P-value*
Pseudomonas fluorescens (G^-)	42 (89%)	11 (100%)	0.024
Campylobacter coli (G^-)	27 (57%)	0 (0%)	4.4E-10
Campylobacter jejuni (G^-)	24 (51%)	0 (0%)	1.2E-08
Enterococcus faecium (G^+)	22 (47%)	0 (0%)	8.3E-08
Malassezia globosa	22 (47%)	10 (91%)	0.001
Pseudomonas protegens (G^-)	18 (38%)	8 (73%)	0.045
Escherichia coli (G^-)	12 (26%)	9 (82%)	0.001
Ralstonia pickettii (G^-)	12 (26%)	8 (73%)	0.008
Pseudomonas aeruginosa (G^-)	11 (23%)	10 (91%)	4.8E-06
Pseudomonas mosselii (G^-)	6 (13%)	9 (82%)	1.4E-04
Bacillus licheniformis (G^+)	6 (13%)	0 (0%)	0.013
Yarrowia lipolytica	5 (11%)	0 (0%)	0.024
Enterobacter cloacae complex (G^-)	3 (6%)	5 (45%)	0.034
Comamonas testosteroni (G^-)	2 (4%)	5 (45%)	0.026
Serratia marcescens (G-)	2 (4%)	5 (45%)	0.026
Stenotrophomonas maltophilia (G^-)	1 (2%)	6 (55%)	0.008
Neisseria sicca (G^-)	0 (0%)	5 (45%)	0.016
Neisseria meningitidis (G^-)	0 (0%)	4 (36%)	0.038
Roseomonas gilardii (G^-)	0 (0%)	4 (36%)	0.038
Staphylococcus capitis (G^+)	0 (0%)	4 (36%)	0.038
* with meibum samples provided. MGD, HC, healthy control; G^+,Gram-positive;G^-Gram-negative.			

Table 2
Pathogens with positive rate over 10% across all meibum samples

Pathogen	#Total meibum samples (n = 58)	MGD (n = 47)	HC (n = 11)	*P*-value
Pseudomonas fluorescens (G^-)	53 (91%)	42 (89%)	11 (100%)	0.02
Cupriavidus metallidurans (G^-)	44 (76%)	36 (77%)	8 (73%)	0.81
Malassezia globosa	32 (55%)	22 (47%)	10 (91%)	8.9E-04
Pseudomonas putida (G^-)	30 (52%)	22 (47%)	8 (73%)	0.12
Campylobacter coli (G^-)	27 (47%)	27 (57%)	0 (0%)	4.4E-10
Pseudomonas protegens (G^-)	26 (45%)	18 (38%)	8 (73%)	0.05
Campylobacter jejuni (G^-)	24 (41%)	24 (51%)	0 (0%)	1.2E-08
Enterococcus faecium (G^+)	22 (38%)	22 (47%)	0 (0%)	8.3E-08
Corynebacterium jeikeium (G^+)	22 (38%)	20 (43%)	2 (18%)	0.10
Alternaria alternata	22 (38%)	16 (34%)	6 (55%)	0.25
Escherichia coli (G^-)	21 (36%)	12 (26%)	9 (82%)	8.6E-04
Pseudomonas aeruginosa (G^-)	21 (36%)	11 (23%)	10 (91%)	4.8E-06
Citrobacter freundii (G^-)	20 (34%)	14 (30%)	6 (55%)	0.17
Ralstonia pickettii (G^-)	20 (34%)	12 (26%)	8 (73%)	0.01
Staphylococcus epidermidis(G^+)	19 (33%)	13 (28%)	6 (55%)	0.14
Corynebacterium simulans (G^+)	18 (31%)	15 (32%)	3 (27%)	0.77
Corynebacterium striatum (G^+)	18 (31%)	15 (32%)	3 (27%)	0.77

Pathogen	#Total meibum samples (n = 58)	MGD (n = 47)	HC (n = 11)	*P*-value
Corynebacterium aurimucosum (G^+)	16 (28%)	13 (28%)	3 (27%)	0.98
Klebsiella pneumoniae (G^-)	15 (26%)	10 (21%)	5 (45%)	0.18
Pseudomonas mosselii (G^-)	15 (26%)	6 (13%)	9 (82%)	1.4E-04
Corynebacterium diphtheriae (G^+)	14 (24%)	11 (23%)	3 (27%)	0.81
Corynebacterium ureicelerivorans (G^+)	11 (19%)	7 (15%)	4 (36%)	0.21
Toxoplasma gondii	10 (17%)	7 (15%)	3 (27%)	0.43
Bacteroides vulgatus (G^-)	10 (17%)	5 (11%)	5 (45%)	0.06
Aeromonas hydrophila (G^-)	9 (16%)	6 (13%)	3 (27%)	0.35
Corynebacterium riegelii (G^+)	7 (12%)	5 (11%)	2 (18%)	0.57
Corynebacterium urealyticum (G^+)	7 (12%)	5 (11%)	2 (18%)	0.57
Bacillus licheniformis (G^+)	6 (10%)	6 (13%)	0 (0%)	0.01
G^+,Gram-positive;G^-Gram-negative.				

Metabolic features of microbiome of MGD meibum and eyelid skin

The assignation results for function annotation in the KEGG list includes the over-represented gene sets at different classification levels in the MGD meibum and eyelid skin. On the other hand, no differential entry was found for conjunctiva (adjusted *p*-value > 0.05, Table S6-S7). Similar to taxonomy profiling, the top 10 gene sets with the largest fold abundance change in the MGD meibum microbiome in each annotation category (Fig. 4A-E) also had significant alterations in the MGD eyelid samples, but not in the MGD conjunctival microbiome. The most notable microbiome changes in both the MGD meibum and eyelid skin were those pathways in mediating microbial metabolism. Among the top 10 KEGG pathways, four were involved in the degradation process including xylene (ko00622), dioxin (ko00621), ethylbenzene (ko00642), and bisphenol (ko00363).

Pathogen	#Total meibum samples (n = 58)	MGD (n = 47)	HC (n = 11)	*P*-value
We further explored the molecular processes underlying 509 enzymes, which were mapped into KEGG pathways. Table S7 lists the enzymes in the MGD meibum microbiome whose abundance increased more than two-fold from their levels in the HC meibum (adjusted *p*-value < 0.05). Over half of them are involved in KEGG Metabolic pathways (63%, 319/509), one hundred of them in biosynthesis of secondary metabolites, 95 others in KEGG pathways of microbial metabolism in diverse environments, and 49 in biosynthesis of antibiotic reference pathways (Table S8). Specifically, all of the 15 pathways involved in carbohydrate metabolism had at least 4 enzymes with increased abundance. The second significant KEGG pathway category is involved with lipid metabolism. Ten out of the 17 pathways contained at least 2 enzymes that were mapped into pathways mediating fatty acid elongation, biosynthesis and degradation, glycerolipid metabolism, glycerophospholipid metabolism, ether lipid metabolism, sphingolipid metabolism, biosynthesis of unsaturated fatty acids, carbon fixation pathways in prokaryotes, and nitrogen metabolism (Table S8).				
For xenobiotic biodegradation and metabolism, 30 enzymes with increased sequencing read abundance mapped into this pathway category. Interestingly, the crucial one was likely mediating benzoate degradation. First, thirteen of these enzymes (43%, 13/30) directly mapped into this pathway (Figure S4A). Second, the subsequent 8 enzymes with increased abundance catalyze the reactions that precede by one or two steps entrance into the benzoate degradation pathway, including E1.14.13.7 (phenol 2-monooxygenase, NADPH) and E1.14.13.82 (vanillate monooxygenase) in aminobenzoate degradation, E3.7.1.8 (2,6-dioxo-6-phenylhexa-3-enoate hydrolase) in dioxin degradation (Figure S4B), E2.3.1.16 (acetyl-CoA C-acyltransferase) in ethylbenzene degradation(Figure S4C), E1.13.11.2 (catechol 2,3-dioxygenase) in styrene degradation (Figure S4D), and E1.14.13.1 (salicylate 1-monooxygenase) in dioxin degradation (Figure S4B), naphthalene degradation (Figure S4E) and polycyclic aromatic hydrocarbon degradation (Figure S4F). In addition, four enzymes involved in the initial step in this process are in a branch leading to benzoate degradation, including E1.1.1.2 (alcohol dehydrogenase, $NADP^+$) and E3.1.1.17 (gluconolactonase) in caprolactam degradation (Figure S4G), E1.14.12.10 (benzoate 1,2-dioxygenase) in fluorobenzoate degradation pathway (Figure S4H) and E4.1.99.11 (benzylsuccinate synthase) in the toluene degradation pathway (Figure S4I).				

Functional features identified in EggNOG database, virulence Factors Database (VFDB) and Antibiotic Resistance Genes Database (ARDB)

EggNOG annotation for contigs obtained in *de novo* assembly demonstrated significantly more functional entries with decreased abundance in the microbiomes of MGD meibum than those in the MGD eyelid skins ($p < 0.0001$, chi-square test, Fig. 5A; details in Table S10-11), which is similar with the observation in taxonomy profiling. The featured virulence factor for MGD meibum microbiome was Type IV secretion system (T4SS), achieving about a 5-fold change in abundance ($q = 0.017$, FDR, Fig. 5B, Table S9). For antibiotic resistance genes, both sites had significantly reduced representation of the FomA gene (Fig. 5C), involved in Fosfomycin resistance.

Discussion

As a result of contact with the external environment, many studies suggest that microbial populations are stable on the ocular surface and in the meibomian gland. Our objective here was to determine the makeup of the microbiome at these sites and also to delineate more extensively their individual microbiota functional features. Such insight was expected to improve our understanding of their microbial metabolic activity and virulence. This could ultimately foster efforts to identify novel effective antibiotic treatment options. In order to reach this goal, microbial population makeup was compared in meibum samples with those at the conjunctiva and in the eyelid skin obtained from individuals with MGD and in HC. The results show that there is a resemblance between the bacterial populations in the meibum and eyelid microbiome. This finding is supportive of speculation indicating that these two sites are connected with one another. Nevertheless, the most significant feature of the MGD meibum microbiome characterization stems from the results of microbial community diversity analysis. It was surprisingly revealed that in the MGD samples there was less pathogen diversity and community richness than in the HC. Finally, our more in-depth analysis of the MGD and HC ocular surface microbiomes shows that there is instead marked disparity between them. Our results are different from others in that the number of bacterial types was significantly higher in the severe MGD group than that in the HC based on 16S rRNA sequencing [19],This disagreement may be attributable to variance in methods and sample size lead Additional studies are warranted work to clarify this discrepancy.

Much effort has been dedicated to perform either whole genome amplification or amplicon sequencing to clarify the identity of the constituents in the microbiome. To satisfy this objective, we developed a protocol to analyze conjunctival microbiomes from contact lens wearers based on 16S rDNA sequencing. Nevertheless, few patients could successfully provide adequate microbiome data of the meibum and two ocular sites. To reduce DNA losses incurred in the extraction process, we did not treat the samples with RNAse before whole genome amplification, which may instead lead to RNA contamination. This difference may explain why the phylum *Negarnaviricota* was present which includes all negative-sense single-stranded RNA viruses in the results (Fig. 2A). However, their read abundance was too small for reliable virus identification. Future ocular virobiome studies may provide novel insights regarding their involvement in eye diseases.

Previous studies reported that the microbial community composition changes with age. This finding is consistent with ours because the skin microbiome constituents were dissimilar between the group aged under 40 years old and the one over 60 years old [20]. To reduce such variance, we enrolled instead young HC volunteers and 42 MGD patients who were under 40 years old. Specifically, the majority of them were not clustered into a HC group for PCA analysis (Fig. 2B). Moreover, the number of pathogens identified in conjunctival and eyelid samples was not age-related (Figure S3). Pathogens *Campylobacter coli*, *Campylobacter jejuni* and *Enterococcus faecium*, which were prevalent in our MGD meibum samples are known to cause eye infections [21–23].

Although there seems to be a negative correlation between the number of pathogens and ocular disease status, this does not mean that MGD patients were at a reduced infection risk. *Pseudomonas fluorescens* was less abundant in MGD meibum (Fig. 3F), but it had the highest positive rate across all meibum

samples (91%, Table 1 and Figure S2E). Nevertheless, infections caused by *P. fluorescens* seem to be rare. They were only detected in a few cases diagnosed with either endophthalmitis [24, 25], bacterial keratitis [26], or infectious crystalline keratopathy [27]. Recently, a study suggested that the routine culture temperature may be too high for *P. fluorescens* to grow, which reduces the likelihood of evaluating its pathogenic impact [28]. For *Pseudomonas putida* abundance, its decline was at a moderate significance level (log_2FoldChange = -1.2, adjusted *p*-value = 0.024) in the MGD meibum compared to its HC counterpart. Whereas, its positive rate was over 50% in meibum samples irrespective of disease status (MGD vs HC, $p = 0.12$, Welch *t*-test, Table S6). *Cupriavidus metallidurans* had a positive rate of 73% in all meibum samples, but it only causes infection under extreme conditions [29]. *Pseudomonas aeruginosa*, a well-known pathogen, which is responsible for 6–39% of bacterial keratitis cases in the United States [30], its positive rate was 40% in our meibum samples; *Staphylococcus epidermidis*, had an positive rate of 48.6% in MGD samples, which was based on the results of a traditional culture method [17] It was present in 33% of the meibum samples irrespective of whether or not they were obtained either from MGD or HC samples (MGD vs HC, $p = 0.17$, Table S6). However, this equivalence may be erroneous due to sample heterogeneity or non-uniform culture methodology among these studies.

The changes in the meibum composition in MGD patients are believed to affect their microbial population makeup. However, almost all significant functional annotation changes identified in MGD meibum were also seen in MGD eyelid skin, indicating that the underlying factors may be shared by the meibomian gland and sebaceous gland. Increased needs for more diverse metabolic pathways in MGD microbiomes may account for the extensive changes in the microenvironment. Fulfillment of bioenergetic requirements of all organisms has top priority, which helps explain why genes promoting carbohydrate related biological processes, carbon fixation and nitrogen metabolism are all over represented (Table S8). The most significant unique metabolic trait of MGD microbiome is its capacity to catabolize benzoate, which belongs to Xenobiotics biodegradation and metabolism in the KEGG database. Most other changes in this pathway category are in agreement with their contribution to switch downstream the reaction direction towards benzoate degradation. Bacterial degradation of benzoate is believed to be part of the biological strategy that underlies the ability of organisms to adapt and survive despite swings in environmental oxygen concentration [31]. This adaptability to survive despite changes in oxygen levels may stem from variations in the composition of MGD meibum.

Microbe profiling alterations may account for how immune cells get activated to increase in abundance to elicit an inflammatory response in tears, in glandular tissue. This cascade of events affects the differentiation of glandular cells and their ability to synthesize and secrete lipids [3]. These inflammatory responses by immune cells in the glandular environment are believed to be a key link in inducing pathological changes. Our study did not identify which microbes exclusively flourish in the MGD meibum. Nevertheless, the microbial community in the MGD samples seems to express more genes that induce chemotaxis and immune evasion (Fig. 5C). Meanwhile, the changes in the meibum composition may also impede the responses by the immune activated cells to eliminate the pathogens in the meibum, which continuously release virulence factors at a stable elevated level. Therefore, MGD meibum harboring a

microbial community containing more Type IV Secretion Systems acts as a sustained intractable stimulant. This notion may partly explain why current efforts in alleviating symptoms are mainly effective if they include procedures that change the meibum composition. This can be accomplished through heating or improving the ability of meibomian glandular cells to produce and release more meibum out of the gland. Additionally, the resemblance between the microbiome composition in the eyelid skin and meibum, makes it apparent that only changing the meibum microbiome may be in vain if similar changes are not also instituted in the eyelid microbiome. Therefore, achieving a more favorable MGD treatment outcome may be realized in the future through altering and monitoring also the eyelid skin microbiome.

Conclusions

Overall, the results demonstrate that MGD meibum has less pathogen diversity and community richness than in the HC, some pathogens were prevalent in MGD meibum samples are known to cause eye infections. There is unique metabolic trait of MGD microbiome, and more genes that induce chemotaxis and immune evasion is expressed in MGD meibum. these findings might increase our understanding of MGD etiology and ultimately have an opportunity to develop potentially novel treatment strategies targeting the microbiota in MGD. Such as being the resemblance between the bacterial populations in the meibum and eyelid microbiome, it may be good strategies for altering and monitoring MGD and also the eyelid skin microbiome for MGD treatment.

Materials And Methods

Recruitment of Subjects

This study was conducted in accordance with the Declaration of Helsinki principles and was approved by Institutional Review Board/Ethics Committee from the Eye Hospital of Wenzhou Medical University (registration number: KYK-2015-01). All of the subjects were recruited at the dry eye center in the Eye Hospital of Wenzhou Medical University and informed consent was obtained from each participant. In this study, 76 volunteers, including 61 patients diagnosed with meibomian gland dysfunction (MGD) and 15 (NC) were enrolled. For all participants, clinical ocular surface examination and symptomatic evaluation were preceded by ophthalmological evaluation at the Dry Eye Center in the Eye Hospital of Wenzhou Medical University, including completion of the McMonnies and ocular surface disease index (OSDI) questionnaire, Schirmer's test for dry eye, tear meniscus height (TMH), tear break up time (TBUT), degree of Meibomian gland absence (upper/ lower) were assessed. Grading of MGD is according to the guideline from the International Workshop on Meibomian Gland Dysfunction [32].

Subject information was obtained, including gender, age, antibiotic usage within 6 months, ocular and general health status. Detailed participant information is shown in Table S1. The inclusion criteria for patients include: (1) patients with complaint of one of the following symptoms: dryness, foreign body sensation, burning; (2) a diagnosis of MGD with two or more of the following signs in both eyes: redness or thickening of the lid margin, telangiectasia, reduced or no secretions, poor quality secretions, and gland

capping; (3) did not have ocular or systemic diseases, ocular traumas, transplantations, or laser surgery; (4) did not recently take antibiotic and/or steroid treatment (within the previous 6-months); (5) did not have allergies to drugs, pollen, etc; (6) no contact lenses were used within the past six months. For normal HC (1) no chief complaint of any dry eye symptoms; (2) MG assessments were not able to meet the criteria for the diagnosis of MGD; (3) corneal staining was negative.

Sampling

All samples were collected from April to September 2017. For each subject, a random eye was chosen for sampling. Firstly, the lower eyelid skin was gently wiped 2–3 times using one Specimen Collection Flocked Swabs (Huachenyang Technology Co., Ltd, Shenzhen, Guangdong, China); the lower bulbar conjunctiva sac of some subjects were also served as an internal control, described as Zhang et al[33]. For sampling of meibomian gland, firstly Proparacaine Hydrochloride (Tianlong Pharmaceutical Co., Ltd, Suzhou, Jiangsu, China) was applied as topical anesthesia, then massaging and pressing the meibomian gland using sterile tweezers, secretion of meibomian gland was collected by Flocked Swabs. The swabs were placed into 1.5 ml tubes (Axygen Biotechnology Co., Ltd, Hangzhou, Zhejiang, China) containing 300 μl DNase-Free ddH2O (Ambion, Thermo Fisher Scientific Inc., Cleveland, OH, USA). The samples were then quickly stored at -80°C until use.

Sequencing experiments

DNA extraction and whole genome amplification followed the protocols described in our previous study [33]. For each sample, 200 ng DNA was used in paired-end sequencing (2 x 150 base pair, bp) on an HiSeq sequencer (Illumina, Inc., San Diego, CA, USA) and 10G raw data were obtained.

Quality Control (QC) of sequencing data

The low-quality bases of the raw reads were trimmed based on the quality information. Trimmomatic (Version 0.36) was used to trim and discard the adaptor sequences [34]. The bases at the beginning and end of each reads were discarded. The Trimmomatic slides from the 5' end in windows with the length at 4 bases; when the average quality in the window is lower than the setting threshold at 15, the read will be cut. The length of reads after QC should be longer than 36 bp.

ribosomal RNA (rRNA) gene depletion for datasets

The SortmeRNA (Version 2.1b) was used to filter the rRNA gene sequence after QC with default parameters and full database (silva-arc-16 s-db, silva-arc-23 s-db, silva-bac-16 s-db,silva-bac-23 s-db,silva-euk-18 s-db,silva-euk-18 s-db,silva-euk-28 s-db,rfam-5.8 s-db,rfam-5 s-db) [35].

Taxonomic assignment of sequencing reads, quantification of taxonomic categories and pathogen identification

The Centrifuge (version 1.0.4b) uses the BWT (Burrows-Wheeler transform) and FM (Ferragina-Manzini) index as the indexing scheme for NCBI NT database (nt_2018_3_3) to classify sequencing reads, and allows each read assigned by multiple taxonomic categories [36]. Then, we assign the read to a single

taxonomic category using the lowest common ancestor of all matching hits with parameters ‘ –min-hitlen 22 -k 1’, We further remove sequencing reads with hit length less than 60 base pairs and assigned to eukaryotic kingdom clade (taxID: 2,759) before taxonomic composition analysis at any taxonomic rank (phylum, class, order, family, genus and species). According to the assigned taxonomic results at the species level, we quantify pathogens in Karius Pathogen List (https://kariusdx.com/pathogenlist/3.4).

Functional profiling of shotgun sequencing reads

The UProc (version 2.0.0-rc1) was used to calculate the functional classification and relative abundance of sequencing reads [37]. Uproc translates DNA into Protein for all the six frames, then compared the reads with oligopeptides at protein-level, and use Mosaic Matching calculation and Mosaic Matching Score to identity the most matching protein family. The SUPER-FOCUS (Version 0.31) was used to annotate with SUPER-FOCUS functional classification system [38]. During annotation, DIAMOND would blast the protein sequence data and fetch The Seed classification information. The antibiotic genes are annotated with ResistoMap with the CARD database for sequence alignment.

De Novo Assembly

Trinity (version 2.8.4) were employed for de novo contig assembly without reference genomes from sequencing reads with parameters ‘–max_memory 300G –min_contig_length 200 –CPU 40 –bflyCPU 40 –inchworm_cpu 40 –full_cleanup –no_normalize_reads’ [39].

Gene function annotation for assembled contigs

The coding sequences in each assembled TRINITY contigs were predicted with MetaProdigal (version 2.6.3) [40]. The COG and KEGG annotation were performed with eggNOG-mapper (version 1.0.3) with eggnog database (version 4.5) [41]. The gene abundance (transcript per million reads, here is gene per million reads) was estimated with Salmon (version 0.11.3) [42]. and the derivations of each functional gene were predicted with Centrifuge, and the antibiotic resistance genes were identified using RGI (version 4.0.2) with CARD database (version 2.0.0) [43]. The proteins with homologous sequences in ARDB database were performed using USEARCH with parameters ‘-b 60 -i 30 -e 1e-10’.

Differential abundance analysis

To identify annotations with differential abundance between the two different groups, the abundance level for each annotation in units of Reads Per Million was calculated using Salmon (version 0.11.3). DESeq2 (version 1.10.1) was used for differential analysis [44]. The between two groups were selected using criteria: *p*-values should be less than 0.05. significant differences in the relative abundance of different taxa present in the bile of both groups were found after the application of the Metastats statistical method with a false discovery rate (FDR correction), adjusted following the Benjamini-Hochberg method.

Data visualization

The PCA and bar-plot figures were generated using R (version R-3.6) [45]. The heatmap figures were generated using pheatmap and ComplexHeatmap packages [46, 47].

Declarations

Acknowledgements

Not applicable

Authors' contributions

F.X.Z., and D.K.Z. interpreted results, and drafted the manuscript. F.X.Z., D.K.Z., and L.Z. performed analyses, developed analysis methods and power calculations. F.X.Z., and C.X.G. enrolled patients and collected all the clinical information. C.C.T. conducted sequencing experiments. F.X.Z., and C.C.T. collected and prepared samples for sequencing analysis, Z.L.Z, C.C.Z., and W.J.F. performed clinical examination and collected results of clinical assays. P.S.R., and C.Q.Z. reviewed and edited the manuscript. X.J.T. interpreted results and provided clinical and bioinformatic expertise. W.C. designed the study, supervised all experiments and analysis, reviewed and edited the manuscript. All authors approved the final version of the manuscript.

Funding

This study is funded by Zhejiang Provincial Natural Science Foundation of China (LY18H120005)
National Natural Science Foundation of China (8157088, and 81970770)
and Innovation Promotion Association CAS (2016098). They have none role in the design of the study and collection, analysis, and interpretation of data and in writing the manuscript.

Availability of data and material

The raw sequence data were deposited in the Genome Sequence Archive in BIG Data Center, Beijing Institute of Genomics (BIG), Chinese Academy of Sciences, under accession numbers PRJCA002217, that are publicly accessible at http://bigd.big.ac.cn/gsa.

Ethics approval and consent to participate

This study was conducted in accordance with the Declaration of Helsinki principles and was approved by Institutional Review Board/Ethics Committee from the Eye Hospital of Wenzhou Medical University (registration number: KYK-2015-01). All of the subjects were recruited at the dry eye center in the Eye Hospital of Wenzhou Medical University and informed consent was obtained from each participant.

Consent for publication

All authors have given consent for publication.

Competing interests

The authors declare no conflict of competing and financial interest.

References

1. Rabensteiner DF, Aminfar H, Boldin I, Schwantzer G, Horwath-Winter J. The prevalence of meibomian gland dysfunction, tear film and ocular surface parameters in an Austrian dry eye clinic population. *Acta Ophthalmol* 2018;96:e707-e11.
2. Knop E, Knop N, Millar T, Obata H, Sullivan DA. The international workshop on meibomian gland dysfunction: report of the subcommittee on anatomy, physiology, and pathophysiology of the meibomian gland. *Invest Ophthalmol Vis Sci* 2011;52:1938-78.
3. Nichols KK, Foulks GN, Bron AJ, Glasgow BJ, Dogru M, Tsubota K, et al. The international workshop on meibomian gland dysfunction: executive summary. *Invest Ophthalmol Vis Sci* 2011;52:1922-9.
4. Arita R, Mori N, Shirakawa R, Asai K, Imanaka T, Fukano Y, et al. Meibum Color and Free Fatty Acid Composition in Patients With Meibomian Gland Dysfunction. *Invest Ophthalmol Vis Sci* 2015;56:4403-12.
5. Pucker AD, Haworth KM. The presence and significance of polar meibum and tear lipids. *Ocul Surf* 2015;13:26-42.
6. Arita R, Mori N, Shirakawa R, Asai K, Imanaka T, Fukano Y, et al. Linoleic acid content of human meibum is associated with telangiectasia and plugging of gland orifices in meibomian gland dysfunction. *Exp Eye Res* 2016;145:359-62.
7. Paranjpe V, Tan J, Nguyen J, Lee J, Allegood J, Galor A, et al. Clinical signs of meibomian gland dysfunction (MGD) are associated with changes in meibum sphingolipid composition. *Ocul Surf* 2019;17:318-26.
8. Green-Church KB, Butovich I, Willcox M, Borchman D, Paulsen F, Barabino S, et al. The international workshop on meibomian gland dysfunction: report of the subcommittee on tear film lipids and lipid-protein interactions in health and disease. *Invest Ophthalmol Vis Sci* 2011;52:1979-93.
9. Graefes Arch Clin Exp OphthalmolHuber-Spitzy V, Baumgartner I, Bohler-Sommeregger K, Grabner G. Blepharitis--a diagnostic and therapeutic challenge. A report on 407 consecutive cases. *Graefes Arch Clin Exp Ophthalmol* 1991;229:224-7.
10. Dougherty JM, Osgood JK, McCulley JP. The role of wax and sterol ester fatty acids in chronic blepharitis. *Invest Ophthalmol Vis Sci* 1991;32:1932-7.
11. Shine WE, McCulley JP. Role of wax ester fatty alcohols in chronic blepharitis. *Invest Ophthalmol Vis Sci* 1993;34:3515-21.
12. Aguiar-Pulido V, Huang W, Suarez-Ulloa V, Cickovski T, Mathee K, Narasimhan G. Metagenomics, Metatranscriptomics, and Metabolomics Approaches for Microbiome Analysis. *Evol Bioinform Online* 2016;12:5-16.

13. Turaev D, Rattei T. High definition for systems biology of microbial communities: metagenomics gets genome-centric and strain-resolved. *Curr Opin Biotechnol* 2016;39:174-81.
14. Sedlar K, Kupkova K, Provaznik I. Bioinformatics strategies for taxonomy independent binning and visualization of sequences in shotgun metagenomics. *Comput Struct Biotechnol J* 2017;15:48-55.
15. Itahashi M, Higaki S, Fukuda M, Shimomura Y. Detection and quantification of pathogenic bacteria and fungi using real-time polymerase chain reaction by cycling probe in patients with corneal ulcer. *Arch Ophthalmol* 2010;128:535-40.
16. Schabereiter-Gurtner C, Maca S, Rolleke S, Nigl K, Lukas J, Hirschl A, et al. 16S rDNA-based identification of bacteria from conjunctival swabs by PCR and DGGE fingerprinting. *Invest Ophthalmol Vis Sci* 2001;42:1164-71.
17. Zhang SD, He JN, Niu TT, Chan CY, Ren CY, Liu SS, et al. Bacteriological profile of ocular surface flora in meibomian gland dysfunction. *Ocul Surf* 2017;15:242-7.
18. Ozkan J, Nielsen S, Diez-Vives C, Coroneo M, Thomas T, Willcox M. Temporal Stability and Composition of the Ocular Surface Microbiome. *Sci Rep* 2017;7:9880.
19. Jiang X, Deng A, Yang J, Bai H, Yang Z, Wu J, et al. Pathogens in the Meibomian gland and conjunctival sac: microbiome of normal subjects and patients with Meibomian gland dysfunction. *Infect Drug Resist* 2018;11:1729-40.
20. Shibagaki N, Suda W, Clavaud C, Bastien P, Takayasu L, Iioka E, et al. Aging-related changes in the diversity of women's skin microbiomes associated with oral bacteria. *Sci Rep* 2017;7:10567.
21. Kuriyan AE, Sridhar J, Flynn HW, Jr., Smiddy WE, Albini TA, Berrocal AM, et al. Endophthalmitis caused by Enterococcus faecalis: clinical features, antibiotic sensitivities, and outcomes. *Am J Ophthalmol* 2014;158:1018-23.
22. Janssen R, Krogfelt KA, Cawthraw SA, van Pelt W, Wagenaar JA, Owen RJ. Host-pathogen interactions in Campylobacter infections: the host perspective. *Clin Microbiol Rev* 2008;21:505-18.
23. Keat A, Rowe I. Reiter's syndrome and associated arthritides. *Rheum Dis Clin North Am* 1991;17:25-42.
24. Robert PY, Chainier D, Garnier F, Ploy MC, Parneix P, Adenis JP, et al. Alcaligenes xylosoxidans endophthalmitis following phacoemulsification and intraocular lens implantation. *Ophthalmic Surg Lasers Imaging* 2008;39:500-4.
25. Essex RW, Charles PG, Allen PJ. Three cases of post-traumatic endophthalmitis caused by unusual bacteria. *Clin Exp Ophthalmol* 2004;32:445-7.
26. Kitzmann AS, Goins KM, Syed NA, Wagoner MD. Bilateral herpes simplex keratitis with unilateral secondary bacterial keratitis and corneal perforation in a patient with pityriasis rubra pilaris. *Cornea* 2008;27:1212-4.
27. Huerva V, Sanchez MC. Infectious crystalline keratopathy caused by Pseudomonas fluorescens. *Eye Contact Lens* 2015;41:e9-e10.

28. Mitra S, Rath S, Das S, Basu S. Ocular infection by a psychrophile: Pseudomonas fluorescens. *Indian J Med Microbiol* 2019;37:289-91.
29. Langevin S, Vincelette J, Bekal S, Gaudreau C. First case of invasive human infection caused by Cupriavidus metallidurans. *J Clin Microbiol* 2011;49:744-5.
30. Sy A, Srinivasan M, Mascarenhas J, Lalitha P, Rajaraman R, Ravindran M, et al. Pseudomonas aeruginosa keratitis: outcomes and response to corticosteroid treatment. *Invest Ophthalmol Vis Sci* 2012;53:267-72.
31. Valderrama JA, Durante-Rodriguez G, Blazquez B, Garcia JL, Carmona M, Diaz E. Bacterial degradation of benzoate: cross-regulation between aerobic and anaerobic pathways. *J Biol Chem* 2012;287:10494-508.
32. Geerling G, Tauber J, Baudouin C, Goto E, Matsumoto Y, O'Brien T, et al. The international workshop on meibomian gland dysfunction: report of the subcommittee on management and treatment of meibomian gland dysfunction. *Invest Ophthalmol Vis Sci* 2011;52:2050-64.
33. Zhang H, Zhao F, Hutchinson DS, Sun W, Ajami NJ, Lai S, et al. Conjunctival Microbiome Changes Associated With Soft Contact Lens and Orthokeratology Lens Wearing. *Invest Ophthalmol Vis Sci* 2017;58:128-36.
34. Bolger AM, Lohse M, Usadel B. Trimmomatic: a flexible trimmer for Illumina sequence data. *Bioinformatics* 2014;30:2114-20.
35. Kopylova E, Noe L, Touzet H. SortMeRNA: fast and accurate filtering of ribosomal RNAs in metatranscriptomic data. *Bioinformatics* 2012;28:3211-7.
36. Kim D, Song L, Breitwieser FP, Salzberg SL. Centrifuge: rapid and sensitive classification of metagenomic sequences. *Genome Res* 2016;26:1721-9.
37. Meinicke P. UProC: tools for ultra-fast protein domain classification. *Bioinformatics* 2015;31:1382-8.
38. Silva GG, Green KT, Dutilh BE, Edwards RA. SUPER-FOCUS: a tool for agile functional analysis of shotgun metagenomic data. *Bioinformatics* 2016;32:354-61.
39. Grabherr MG, Haas BJ, Yassour M, Levin JZ, Thompson DA, Amit I, et al. Full-length transcriptome assembly from RNA-Seq data without a reference genome. *Nat Biotechnol* 2011;29:644-52.
40. Hyatt D, LoCascio PF, Hauser LJ, Uberbacher EC. Gene and translation initiation site prediction in metagenomic sequences. *Bioinformatics* 2012;28:2223-30.
41. Huerta-Cepas J, Forslund K, Coelho LP, Szklarczyk D, Jensen LJ, von Mering C, et al. Fast Genome-Wide Functional Annotation through Orthology Assignment by eggNOG-Mapper. *Mol Biol Evol* 2017;34:2115-22.
42. Patro R, Duggal G, Love MI, Irizarry RA, Kingsford C. Salmon provides fast and bias-aware quantification of transcript expression. *Nat Methods* 2017;14:417-9.
43. Alcock BP, Raphenya AR, Lau TTY, Tsang KK, Bouchard M, Edalatmand A, et al. CARD 2020: antibiotic resistome surveillance with the comprehensive antibiotic resistance database. *Nucleic Acids Res* 2020;48:D517-D25.

44. Love MI, Huber W, Anders S. Moderated estimation of fold change and dispersion for RNA-seq data with DESeq2. *Genome Biol* 2014;15:550.
45. Team RC. R: A language and environment for statistical computing. 2013.
46. Gu Z, Eils R, Schlesner M. Complex heatmaps reveal patterns and correlations in multidimensional genomic data. *Bioinformatics* 2016;32:2847-9.
47. Kolde R, Kolde MR. Package 'pheatmap'. *R Package* 2015;1.

f meibomian gland dysfunction, tear film and ocular surface parameters in an Austrian dry eye clinic population. Acta Ophthalmol. 2018;96:e707-e11.

- Knop E, Knop N, Millar T, Obata H, Sullivan DA. The international workshop on meibomian gland dysfunction: report of the subcommittee on anatomy, physiology, and pathophysiology of the meibomian gland. *Invest Ophthalmol Vis Sci* 2011;52:1938-78.
- Nichols KK, Foulks GN, Bron AJ, Glasgow BJ, Dogru M, Tsubota K, et al. The international workshop on meibomian gland dysfunction: executive summary. *Invest Ophthalmol Vis Sci* 2011;52:1922-9.
- Arita R, Mori N, Shirakawa R, Asai K, Imanaka T, Fukano Y, et al. Meibum Color and Free Fatty Acid Composition in Patients With Meibomian Gland Dysfunction. Invest Ophthalmol Vis Sci. 2015;56:4403–12.
- Pucker AD, Haworth KM. The presence and significance of polar meibum and tear lipids. Ocul Surf. 2015;13:26–42.
- Arita R, Mori N, Shirakawa R, Asai K, Imanaka T, Fukano Y, et al. Linoleic acid content of human meibum is associated with telangiectasia and plugging of gland orifices in meibomian gland dysfunction. Exp Eye Res. 2016;145:359–62.
- Paranjpe V, Tan J, Nguyen J, Lee J, Allegood J, Galor A, et al. Clinical signs of meibomian gland dysfunction (MGD) are associated with changes in meibum sphingolipid composition. Ocul Surf. 2019;17:318–26.
- Green-Church KB, Butovich I, Willcox M, Borchman D, Paulsen F, Barabino S, et al. The international workshop on meibomian gland dysfunction: report of the subcommittee on tear film lipids and lipid-protein interactions in health and disease. *Invest Ophthalmol Vis Sci* 2011;52:1979-93.
- Graefes Arch Clin Exp. OphthalmolHuber-Spitzy V, Baumgartner I, Bohler-Sommeregger K, Grabner G. Blepharitis–a diagnostic and therapeutic challenge. A report on 407 consecutive cases. Graefes Arch Clin Exp Ophthalmol 1991;229:224–7.
- Dougherty JM, Osgood JK, McCulley JP. The role of wax and sterol ester fatty acids in chronic blepharitis. Invest Ophthalmol Vis Sci. 1991;32:1932–7.
- Shine WE, McCulley JP. Role of wax ester fatty alcohols in chronic blepharitis. Invest Ophthalmol Vis Sci. 1993;34:3515–21.
- Aguiar-Pulido V, Huang W, Suarez-Ulloa V, Cickovski T, Mathee K, Narasimhan G. Metagenomics, Metatranscriptomics, and Metabolomics Approaches for Microbiome Analysis. Evol Bioinform

Online. 2016;12:5–16.

- Turaev D, Rattei T. High definition for systems biology of microbial communities: metagenomics gets genome-centric and strain-resolved. Curr Opin Biotechnol. 2016;39:174–81.
- Sedlar K, Kupkova K, Provaznik I. Bioinformatics strategies for taxonomy independent binning and visualization of sequences in shotgun metagenomics. Comput Struct Biotechnol J. 2017;15:48–55.
- Itahashi M, Higaki S, Fukuda M, Shimomura Y. Detection and quantification of pathogenic bacteria and fungi using real-time polymerase chain reaction by cycling probe in patients with corneal ulcer. Arch Ophthalmol. 2010;128:535–40.
- Schabereiter-Gurtner C, Maca S, Rolleke S, Nigl K, Lukas J, Hirschl A, et al. 16S rDNA-based identification of bacteria from conjunctival swabs by PCR and DGGE fingerprinting. Invest Ophthalmol Vis Sci. 2001;42:1164–71.
- Zhang SD, He JN, Niu TT, Chan CY, Ren CY, Liu SS, et al. Bacteriological profile of ocular surface flora in meibomian gland dysfunction. Ocul Surf. 2017;15:242–7.
- Ozkan J, Nielsen S, Diez-Vives C, Coroneo M, Thomas T, Willcox M. Temporal Stability and Composition of the Ocular Surface Microbiome. Sci Rep. 2017;7:9880.
- Jiang X, Deng A, Yang J, Bai H, Yang Z, Wu J, et al. Pathogens in the Meibomian gland and conjunctival sac: microbiome of normal subjects and patients with Meibomian gland dysfunction. Infect Drug Resist. 2018;11:1729–40.
- Shibagaki N, Suda W, Clavaud C, Bastien P, Takayasu L, Iioka E, et al. Aging-related changes in the diversity of women's skin microbiomes associated with oral bacteria. Sci Rep. 2017;7:10567.
- Kuriyan AE, Sridhar J, Flynn HW Jr, Smiddy WE, Albini TA, Berrocal AM, et al. Endophthalmitis caused by Enterococcus faecalis: clinical features, antibiotic sensitivities, and outcomes. Am J Ophthalmol. 2014;158:1018–23.
- Janssen R, Krogfelt KA, Cawthraw SA, van Pelt W, Wagenaar JA, Owen RJ. Host-pathogen interactions in Campylobacter infections: the host perspective. Clin Microbiol Rev. 2008;21:505–18.
- Keat A, Rowe I. Reiter's syndrome and associated arthritides. Rheum Dis Clin North Am. 1991;17:25–42.
- Robert PY, Chainier D, Garnier F, Ploy MC, Parneix P, Adenis JP, et al. Alcaligenes xylosoxidans endophthalmitis following phacoemulsification and intraocular lens implantation. Ophthalmic Surg Lasers Imaging. 2008;39:500–4.
- Essex RW, Charles PG, Allen PJ. Three cases of post-traumatic endophthalmitis caused by unusual bacteria. Clin Exp Ophthalmol. 2004;32:445–7.
- Kitzmann AS, Goins KM, Syed NA, Wagoner MD. Bilateral herpes simplex keratitis with unilateral secondary bacterial keratitis and corneal perforation in a patient with pityriasis rubra pilaris. Cornea. 2008;27:1212–4.
- Huerva V, Sanchez MC. Infectious crystalline keratopathy caused by Pseudomonas fluorescens. Eye Contact Lens. 2015;41:e9–10.

- Mitra S, Rath S, Das S, Basu S. Ocular infection by a psychrophile: Pseudomonas fluorescens. Indian J Med Microbiol. 2019;37:289–91.
- Langevin S, Vincelette J, Bekal S, Gaudreau C. First case of invasive human infection caused by Cupriavidus metallidurans. J Clin Microbiol. 2011;49:744–5.
- Sy A, Srinivasan M, Mascarenhas J, Lalitha P, Rajaraman R, Ravindran M, et al. Pseudomonas aeruginosa keratitis: outcomes and response to corticosteroid treatment. Invest Ophthalmol Vis Sci. 2012;53:267–72.
- Valderrama JA, Durante-Rodriguez G, Blazquez B, Garcia JL, Carmona M, Diaz E. Bacterial degradation of benzoate: cross-regulation between aerobic and anaerobic pathways. J Biol Chem. 2012;287:10494–508.
- Geerling G, Tauber J, Baudouin C, Goto E, Matsumoto Y, O'Brien T, et al. The international workshop on meibomian gland dysfunction: report of the subcommittee on management and treatment of meibomian gland dysfunction. *Invest Ophthalmol Vis Sci* 2011;52:2050-64.
- Zhang H, Zhao F, Hutchinson DS, Sun W, Ajami NJ, Lai S, et al. Conjunctival Microbiome Changes Associated With Soft Contact Lens and Orthokeratology Lens Wearing. Invest Ophthalmol Vis Sci. 2017;58:128–36.
- Bolger AM, Lohse M, Usadel B. Trimmomatic: a flexible trimmer for Illumina sequence data. Bioinformatics. 2014;30:2114–20.
- Kopylova E, Noe L, Touzet H. SortMeRNA: fast and accurate filtering of ribosomal RNAs in metatranscriptomic data. Bioinformatics. 2012;28:3211–7.
- Kim D, Song L, Breitwieser FP, Salzberg SL. Centrifuge: rapid and sensitive classification of metagenomic sequences. Genome Res. 2016;26:1721–9.
- Meinicke P. UProC: tools for ultra-fast protein domain classification. Bioinformatics. 2015;31:1382–8.
- Silva GG, Green KT, Dutilh BE, Edwards RA. SUPER-FOCUS: a tool for agile functional analysis of shotgun metagenomic data. Bioinformatics. 2016;32:354–61.
- Grabherr MG, Haas BJ, Yassour M, Levin JZ, Thompson DA, Amit I, et al. Full-length transcriptome assembly from RNA-Seq data without a reference genome. Nat Biotechnol. 2011;29:644–52.
- Hyatt D, LoCascio PF, Hauser LJ, Uberbacher EC. Gene and translation initiation site prediction in metagenomic sequences. Bioinformatics. 2012;28:2223–30.
- Huerta-Cepas J, Forslund K, Coelho LP, Szklarczyk D, Jensen LJ, von Mering C, et al. Fast Genome-Wide Functional Annotation through Orthology Assignment by eggNOG-Mapper. Mol Biol Evol. 2017;34:2115–22.
- Patro R, Duggal G, Love MI, Irizarry RA, Kingsford C. Salmon provides fast and bias-aware quantification of transcript expression. Nat Methods. 2017;14:417–9.
- Alcock BP, Raphenya AR, Lau TTY, Tsang KK, Bouchard M, Edalatmand A, et al. CARD 2020: antibiotic resistome surveillance with the comprehensive antibiotic resistance database. Nucleic

Acids Res. 2020;48:D517-D25.
- Love MI, Huber W, Anders S. Moderated estimation of fold change and dispersion for RNA-seq data with DESeq2. Genome Biol. 2014;15:550.
- Team RC. R: A language and environment for statistical computing. 2013.
- Gu Z, Eils R, Schlesner M. Complex heatmaps reveal patterns and correlations in multidimensional genomic data. Bioinformatics. 2016;32:2847–9.
- Kolde R, Kolde MR. Package 'pheatmap'. *R Package* 2015;1.

Additional Files

Additional file 1: Supplemental 5 figures and 11 tables. **Figure S1.** Principal Component Analysis at different taxonomic classifications according to results using Centrifuge (**A**) and Metaphlan2 (**B**). **Figure S2.** Pathogens detected in the meibum obtained from MGD patients and HC samples. Comparisons of pathogen numbers detected in meibum, eyelid skin and conjunctiva **(A)**, patients with different MGD grades **(B)**, and genders **(C)**. Pathogens in each meibum sample(**D**), have differential incidence among patients with different MGD grades and HC. (**E**) Pathogens with incidence over 10% across all meibum samples. Abbreviations: MGD, Meibomian gland dysfunction; HC, health controls; MM, MGD meibum. **Figure S3.** Correlation between number of Pathogens detected in samples and age of patients or healthy volunteers. **Figure S4.** Mapping of KEGG enzymes to pathways in Xenobiotics biodegradation and metabolism. **A.** Benzoate degradation; **B.** Dioxin degradation; **C.** Ethylbenzene degradation; **D.** Styrene degradation; **E.** Naphthalene degradation; **F.** Polycyclic aromatic hydrocarbon degradation; **G.** Caprolactam degradation; **H.** Fluorobenzoate degradation; **I.** Toluene degradation. **Table S1**. clinical Data. **Table S2**. sequencing statistics. **Table S3**. contig summarization. **Table S4**. significant taxa changes in MGD meibum. **Table S5**. significant taxa changes in MGD eyelid skin. **Table S6**. KEGG Meibum.sig. **Table S7**. KEGG eyelid skin.sig. **Table S8**. Mapping of KEGG enzymes to pathways. **Table S9**. annotation of top KEEG ID. **Table S10**. meibum_Eggnogg_VFDB_ARDB. T**able S11**. eyelid_Eggnogg_VFDB_ARDB.

Figures

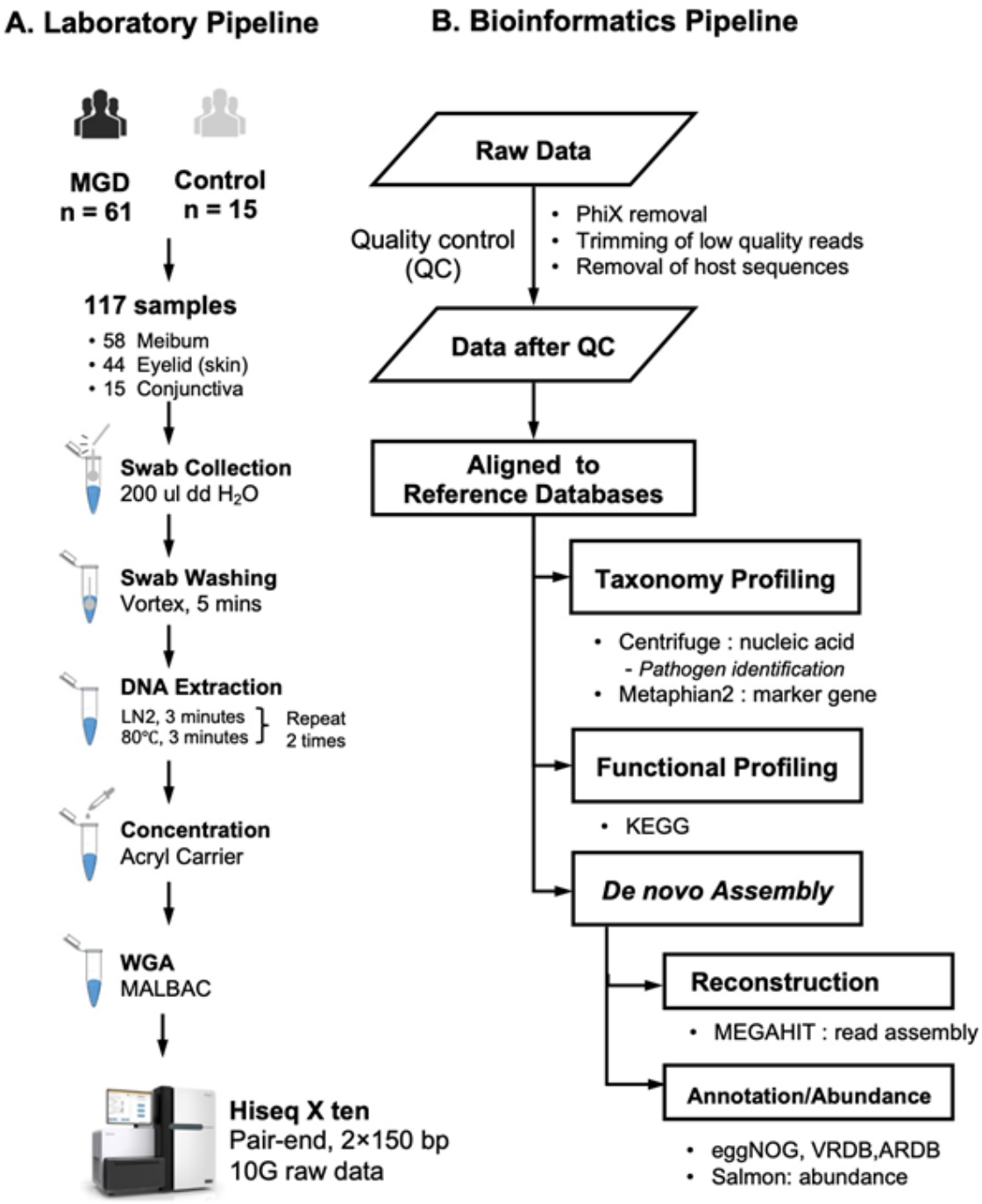

Figure 1

Study design. (A) Laboratory Pipeline. Swabs were collected from 76 subjects, including 61 MGD patients and 15 HC volunteers. Totally, 117 samples had qualified sequencing results (Method), including 58 were from meibum, 44 from skin of eyelid, and 15 from conjunctiva. Liquid nitrogen (LN) was used for DNA extraction, and Acryl carrier was used to enrich the DNA fragment and decrease the volumes of DNA solution. Whole genome amplification (WGA) was applied to obtain adequate amount of DNA for

sequencing library construction. (B) Bioinformatic Pipeline. Quality control process low quality reads, PhiX and host sequences were removed in the quality control process. Multiple tools and public databases were applied to annotate sequencing fragments and de novo assembly.

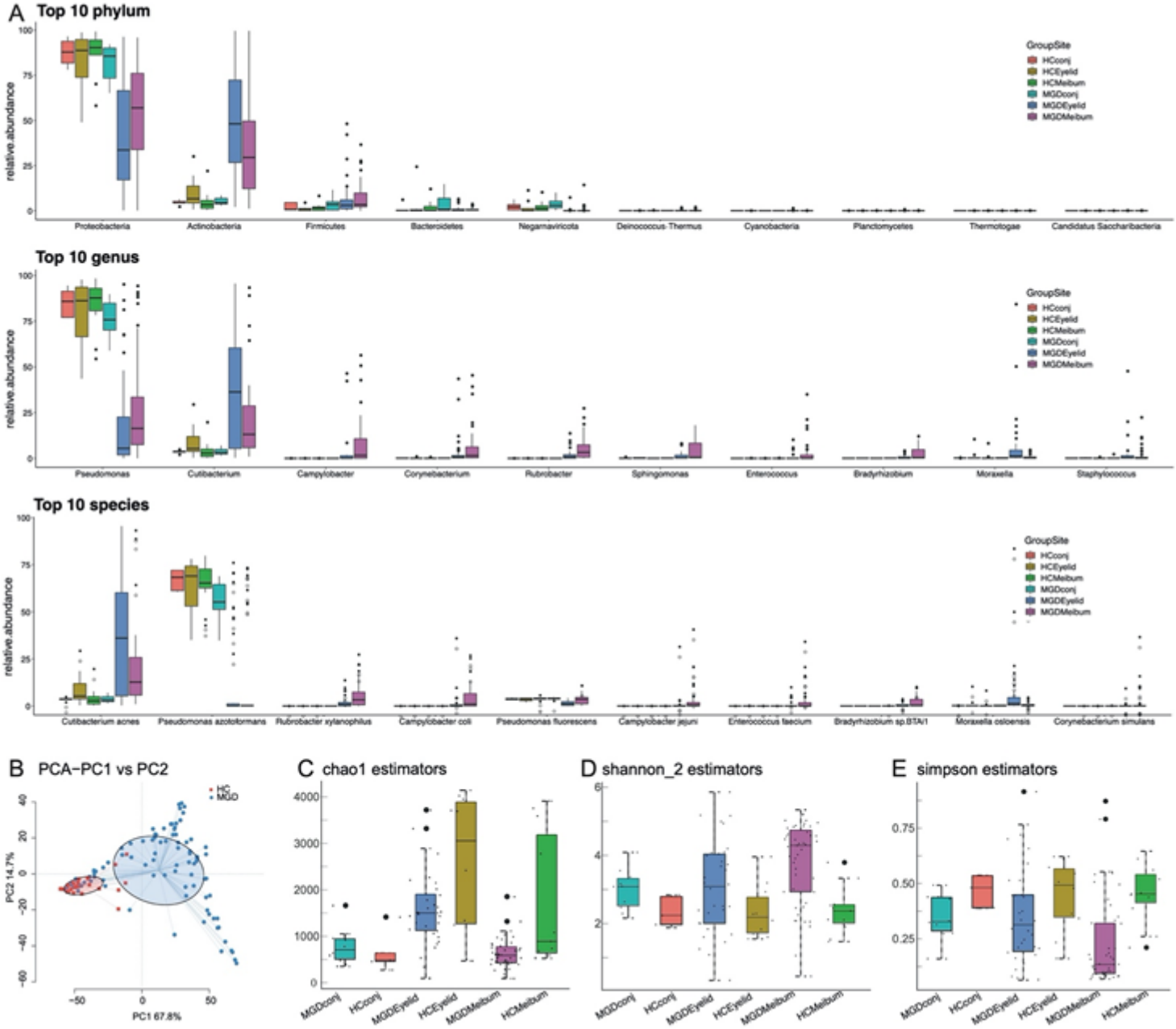

Figure 2

Overall comparison of taxonomic classification in microbiome of all samples. (A) Microbial diversity in meibum, eyelid skin and conjunctiva. (B) Principle coordinate analysis (PCoA) plot of microbial communities at genus level (centrifuge). Alpha diversity (C-E) measured by KO abundance for MGD patients and HC individuals.

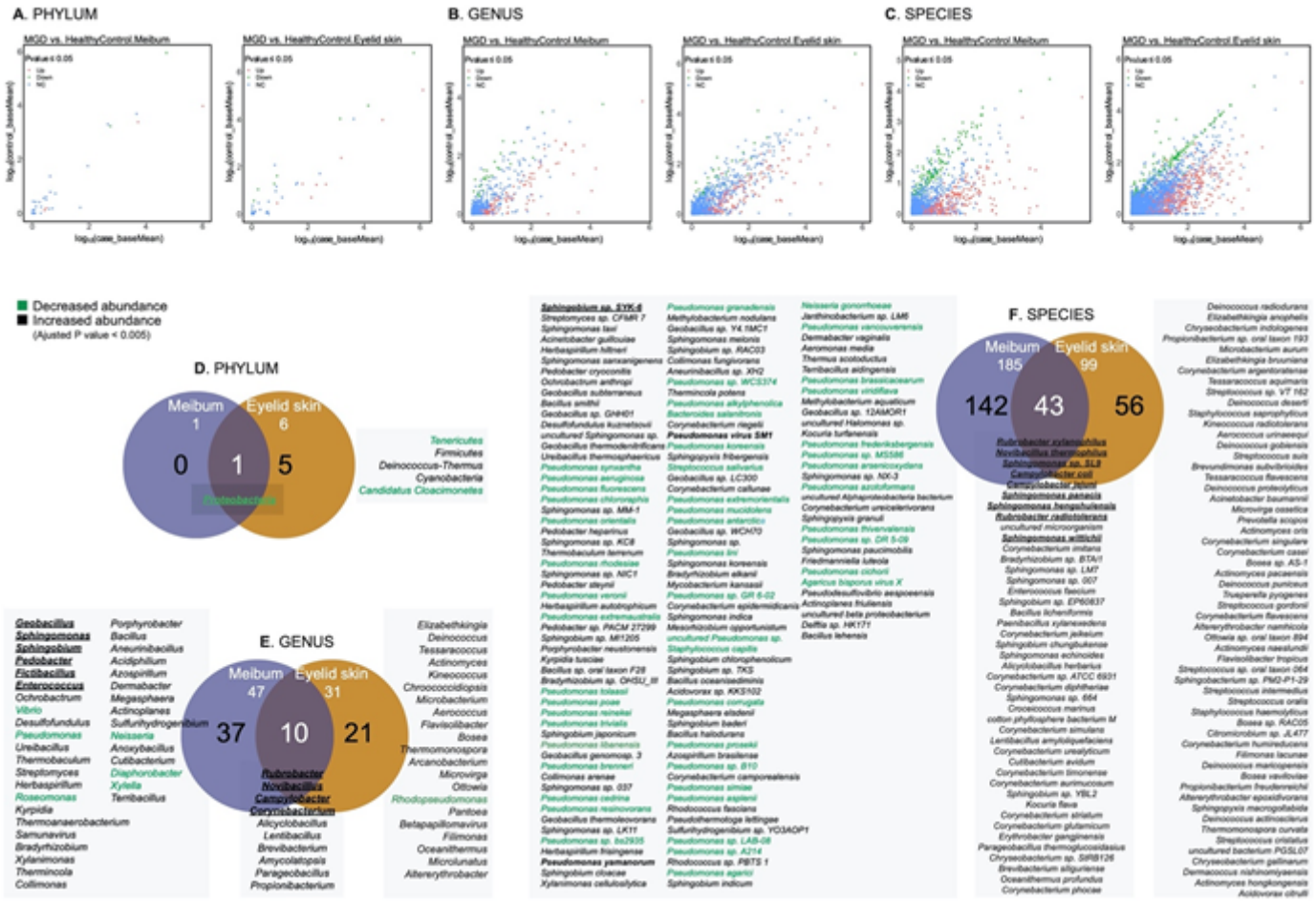

Figure 3

Comparison of significant changes at the different taxonomic levels in meibum and eyelid microbiomes of MGD patients. Dot plots show the mean abundance of each taxa in different classifications (A: phylum, B: genus, C: species) in MGD patients (x axis) and HC (healthy control) individuals (y axis). The colors of dots indicate if the taxon has a significantly higher (red)/lower (green) abundance in MGD patients ($p < 0.05$, Welch t-test), or their abundance is at similar levels in MGD and HC groups (blue). Venn plots show the common and specific taxa with most significant abundance changes (adjusted p-value < 0.005, Benjamini-Hochberg) in microbiomes from meibum and eyelid skin of MGD patients. The taxa shown in green have significantly lower abundance in MGD meibum. Bold italics denote top 10 taxa with differential abundance in the MGD meibum microbiome. The taxa ranking is based on their significance level.

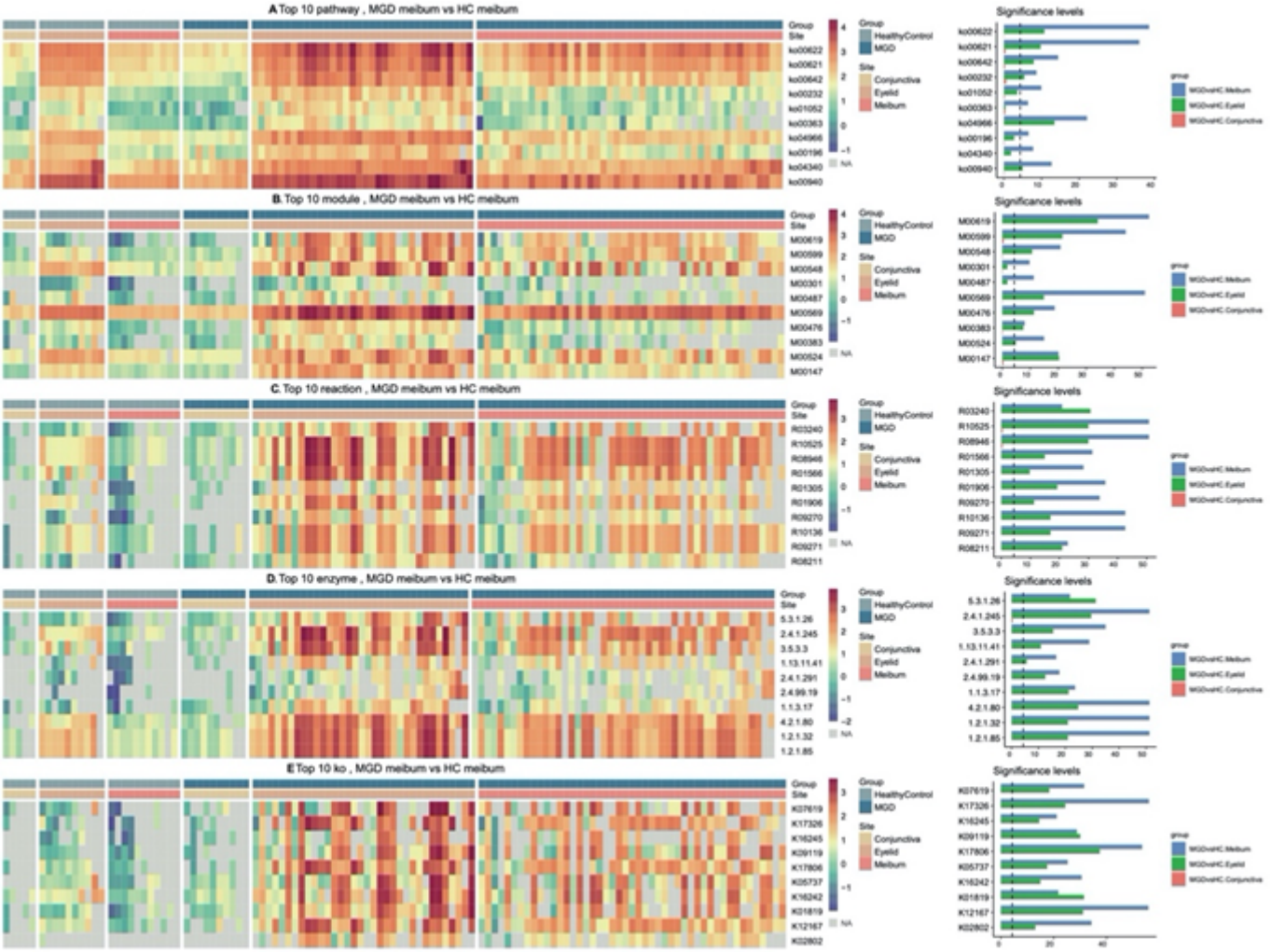

Figure 4

Over-representation of functions in microbiomes from MGD patients and HC. Annotations according to KEGG database at different layers: (A) Pathway; (B) Module; (C) Reaction; (D) Enzyme; (E) KEGG Orthology, KO. Full annotations for each entry are listed in Table S9. The rank of top ten entries is listed in a descending order according to fold change of abundance in MGD meibum. Right panel: X axis, -log2(adjust p-value), dashed vertical line: adjust p-value = 0.05.

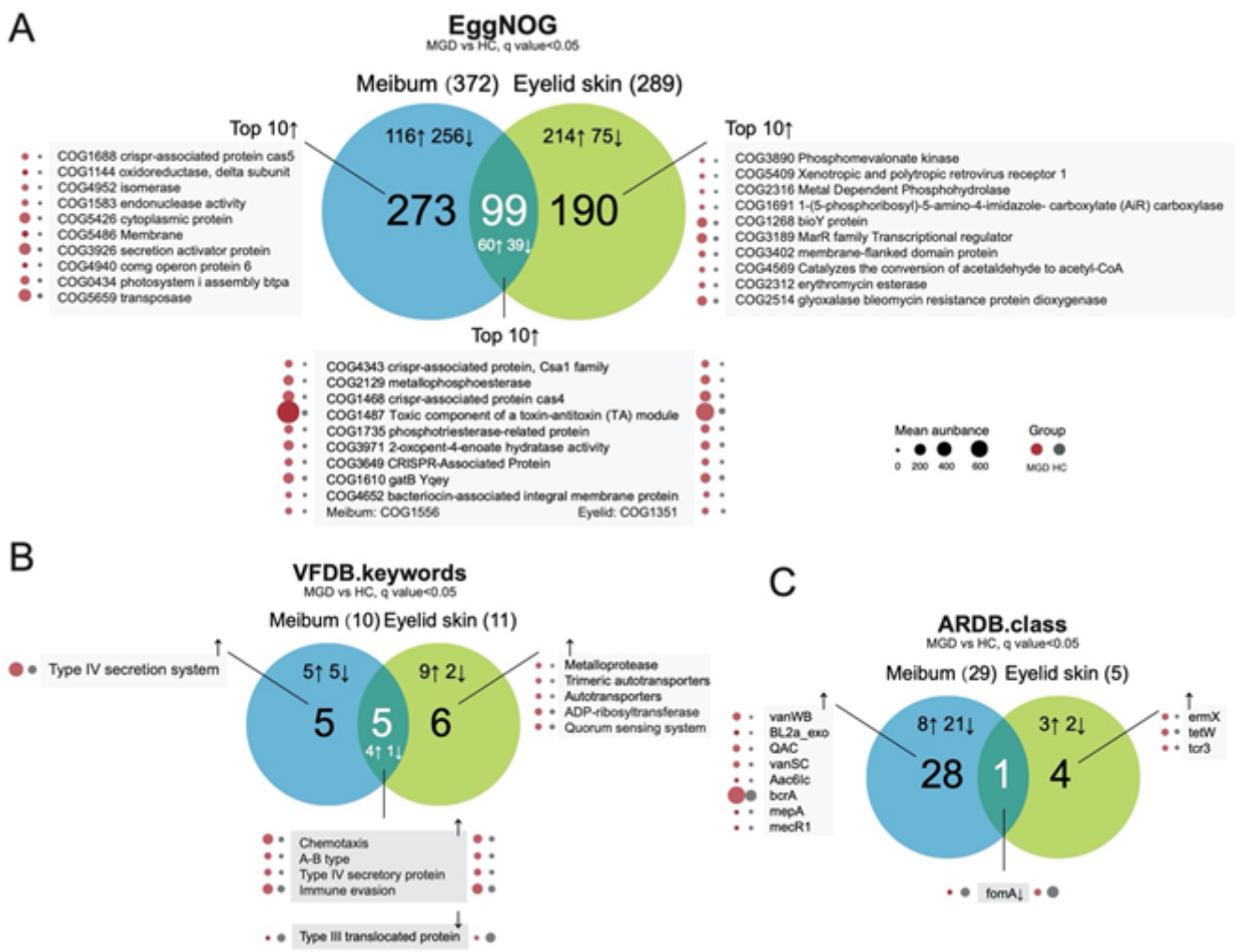

Figure 5

Over-representation of functional entries in (A) EggNOG (evolutionary genealogy of genes: Non-supervised Orthologous Groups) database, (B) virulence Factors Database (VFDB) and (C) Antibiotic Resistance Genes Database (ARDB) in microbiomes of MGD meibum and eyelid skin. ↑ increase; ↓ decrease.

Supplementary Files

This is a list of supplementary files associated with this preprint. Click to download.

- TableS7KEGGeyelidskin.sig.xlsx
- TableS2sequencingstatistics.xlsx
- TableS8MappingofKEGGenzymestopathways.xlsx
- TableS4significanttaxachangesinMGDmeibum.xlsx
- MGDSupplementaryFigures20200413.pdf
- TableS6KEGGMeibum.sig.xlsx

- TableS9annotationoftopKEEGID.xlsx
- TableS11eyelidEggnoggVFDBARDB.xlsx
- TableS3contigsummarization.xlsx
- TableS5significanttaxachangesinMGDeyelidskin.xlsx
- TableS1clinicalData.xlsx
- TableS10meibumEggnoggVFDBARDB.xlsx